FUEL SLOSHING STUDIES

Prepared by

H. Norman Abramson
Luis R. Garza
Daniel D. Kana

Prepared for

National Aeronautics & Space Administration
George C. Marshall Space Flight Center
Huntsville, Alabama

GPO PRICE $ _____

CFSTI PRICE(S) $ _____

Hard copy (HC) _____

Microfiche (MF) _____

H 653 July 65

Quarterly Progress Report No. 3
Contract No. NAS8-1555
SwRI Project No. 1072-2

January 1, 1962

N66 32645

(ACCESSION NUMBER)   (THRU)

(PAGES)   (CODE)

(NASA CR OR TMX OR AD NUMBER)   (CATEGORY)

FACILITY FORM 602

SOUTHWEST RESEARCH INSTITUTE

SAN ANTONIO, TEXAS

S O U T H W E S T R E S E A R C H I N S T I T U T E
8500 Culebra Road, San Antonio 6, Texas

Department of Mechanical Sciences
Engineering Analysis Section

FUEL SLOSHING STUDIES

Prepared by

H. Norman Abramson
Luis R. Garza
Daniel D. Kana

Prepared for

National Aeronautics & Space Administration
George C. Marshall Space Flight Center
Huntsville, Alabama

Quarterly Progress Report No. 3
Contract No. NAS8-1555
SwRI Project No. 1072-2

January 1, 1962

APPROVED:

H. Norman Abramson, Director
Department of Mechanical Sciences

TABLE OF CONTENTS

ABSTRACT

$3\ 2\ 6\ 4\ 5$

This report presents the results of experiments conducted with sloshing liquids in cylindrical and spherical tanks during the period 1 October 1961 through 1 January 1962.

Tests were performed to determine the effect of baffle location on the damping produced by a single fixed ring baffle in a cylindrical tank with constant liquid depth. Resulting forced vibration damping factors are compared with free vibration damping factors obtained by NASA. Experiments with spherical tanks were performed to determine total force response for bare wall and ring baffled tanks. The spherical tanks were excited both in translation and in pitching.

author

LIST OF SYMBOLS

F	Total resultant force of liquid exerted on tank
ρ	Liquid density
a	Longitudinal acceleration of tank
d	Cylindrical or spherical tank major diameter
X_o	Tank excitation amplitude in translation
ω	Circular frequency of tank excitation
ω_n	Liquid natural circular frequency
ϕ	Phase angle between total force and tank displacement
μ	Liquid viscosity
R	Cylindrical or spherical tank major radius
d_s	Distance from top of baffle to liquid surface
W	Baffle width
h	Liquid depth to bottom of tank
δ	Logarithmic decrement damping factor
g	Half bandwidth damping factor
$\dfrac{F}{\rho a d^3 (X_o/d)}$	Dimensionless force amplitude
$\dfrac{\omega^2 d}{a}$	Dimensionless frequency parameter

LIST OF ILLUSTRATIONS

I. INTRODUCTION

The results of total force response measurements obtained from sloshing tests of water and methylene chloride in a 90° sector tank having solid or perforated sector walls were presented in Quarterly Progress Reports No. 1 and No. 2 (1,2)[*]. The correlation of this data with theory is still pending the receipt of theoretical data from Marshall Space Flight Center.

The results presented in the present report were obtained from similar experiments conducted in a 14.4-in. diameter <u>cylindrical</u> tank and in a 14.5-in. diameter <u>spherical</u> tank. The cylindrical tank was utilized to investigate the variation in total force amplitude damping as a result of changing the baffle-to-liquid surface location of a single fixed ring baffle. It was desired to compare resulting forced vibration damping factors with free vibration damping factors obtained by NASA using moment amplitude logarithmic decrement (3). Upon completion of the work on the cylindrical tank, the facility was converted for sloshing studies in the spherical tank. The results of measurements of the total force response for a bare wall tank and tanks with two different baffle configurations are presented in the present report.

---

[*] Numbers in parentheses denote references cited at the end of this report.

During the current period, additional funds were received to broaden somewhat the scope of the contract. The above mentioned study of ring baffle damping in a cylindrical tank partially fulfills these additional requirements.

II. PROGRESS DURING CURRENT QUARTER

A.   Damping Produced by a Ring Baffle Fixed at Various Levels
in a Cylindrical Tank

1.   Description of Experimental Apparatus. The same test

facility and basic tank employed in the 90° sector tank studies was

used in conducting these experiments. The ring baffle installed for

this investigation was made of 12 ga. (0.1046) solid steel with a baffle

width-to-tank radius (W/R) ratio of 0.157. The baffle was secured in

the tank by four 1/8" x 3/4" steel strips that were welded flush at 90°

apart to the outer edge of the ring, and were supported through angle

iron brackets bolted to the upper flange of the tank, as shown in Fig-

ure 1. Successive holes were drilled in the strips to locate the baffle

accurately at surface distance to tank radius (d_s/R) values ranging

from 0.025 to 0.70.   The support strips were considered small

enough in cross section and properly located so that they had no appre-

ciable effect on damping characteristics.

2.   Experimental Results. The damping factors obtained from

these forced vibration tests are shown in Figure 2, where a comparison

is made with the results of NASA tests of a ring baffle with the same

W/R ratio, but in a 12-in. diameter tank undergoing free vibration.

The NASA results are taken from Figure 4 of Ref. (3). In comparing

these results, it must be kept in mind that the SwRI method of obtaining

damping factors is different from that utilized by NASA. In the SwRI method, the damping factor g is evaluated from experimental force response data for forced vibration at each value of d_s/R using the half bandwidth technique developed by Bauer (4). The damping factor δ, presented by NASA, is determined from the moment amplitude logarithmic decrement from free vibration. It can be shown that the two factors are related by

$$\delta = \pi g$$

Figure 2 presents the comparison in terms of the NASA damping factor δ.

Basically, both methods appear to give the same general variation of damping with baffle location. In particular, both show that maximum damping occurs for depth ratios in the vicinity of $d_s/R = 0.08$. The magnitude of the SwRI damping factor is different, however, over some portions of the depth range. This difference is probably a result of the dependence of damping on free surface oscillation amplitude. The NASA procedure included measuring moment amplitude decay using a fixed initial reference moment for each value of d_s/R. This reference moment was established by varying the initial free surface oscillation amplitude, which was excited with a paddle prior to making the free vibration measurements. The reference moment chosen was slightly below the maximum moment

for which the fundamental mode could be defined for the wide variety of

baffles and test conditions employed. Since several different types of

baffles were investigated, the limiting condition was probably that which

employed the baffle producing the least damping. With this particular

baffle, breaking waves would most likely occur for liquid surface ampli-

tudes corresponding to the reference moment. For certain other baffles

and test conditions for which relatively high damping existed, it was

necessary to employ a somewhat greater liquid surface amplitude to

produce the reference moment.

The SwRI experiments were all conducted using a constant excita-

tion amplitude in translation, therefore the liquid free surface oscillations

could grow to larger amplitudes as the damping decreased. It was also

shown by NASA (3) that damping increases with liquid free surface am-

plitude, at least in the vicinity of $d_s/R = 0.333$, but unfortunately the

data given is only for comparatively small amplitudes. Evidence has

been presented elsewhere (5) that damping produced by fixed ring baffles

generally increases with increasing excitation amplitude; it is believed

that this increase continues until virtually complete damping loss occurs

at large amplitudes of liquid oscillation, where breaking waves and rota-

tional motion predominate.

This general behavior probably explains the difference in damping

factors shown in Figure 2, for the range $d_s/R > 0.125$ and at the optimum

point d_s/R = 0. 08. In both the SwRI and NASA tests, damping would

tend to decrease with increasing d_s/R > 0. 125, and force and moment

would tend to increase. This reduction in damping in the SwRI tests

was not as great as that of NASA since liquid free surface oscillation

amplitude was not controlled. The liquid amplitude increased with

constant excitation amplitude and increasing depth ratios, up to d_s/R =

0. 38; at this point it was observed that breaking waves and rotational

motion occurred, so that virtually a complete loss of damping resulted

and the force response curves show a sharp break. In order to obtain

any damping data in this range, it would be necessary to reduce the

constant translational excitation amplitude so that a family of curves

would result, one for each constant value of excitation amplitude.

Near the optimum baffle location d_s/R = 0. 08, the increase of damping

with free surface oscillation amplitude again apparently caused the

difference in damping factors; however, at this point the NASA factor

is greater. In this case, the NASA tests required larger liquid sur-

face amplitudes to produce the initial reference moment, hence,

additional damping resulted. It should be noted that the NASA data is

presented as an average of a comparatively wide scatter of values.

In general, it can be stated that both studies resulted in similar

behavior of damping factor with baffle depth. It would probably be

desirable to obtain a family of damping curves for various excitation

amplitudes so that the effects of free surface amplitude would be included. The NASA data show the effects of the free surface amplitude only at the point of optimum damping; the damping at this point might be yet greater with a further increase in free surface amplitude.

It is of interest to note that a theoretical analysis for a single ring baffle has been carried out by Miles (6). The damping factor can be shown to take the form

$$\delta = \phi_L K \frac{W}{R}\left(2 - \frac{W}{R}\right) e^{-5.52 \frac{d_s}{R}}$$

where ϕ_L is the slope of the liquid free surface and K is an arbitrary constant. For a constant free surface amplitude ϕ_L, the value of damping factor continually decreases with increasing d_s/R. It is not possible to make a direct comparison between this theory and the experimental data presented in Figure 2 because data on the value of ϕ_L is not available for either the NASA or SwRI tests. Comparisons between this theory and other experiments (for K = 7.5) have been given in Refs. (6) and (7).

A comparison with the results of NASA tests on the effect of baffle location on fundamental resonant sloshing frequency in the cylindrical tank is shown in Figure 3. The natural frequency is plotted in the non-dimensional form $\omega_n^2 d/a$, as has been done previously in all SwRI work. The NASA results are based on data presented

in Figure 13 of Ref. (3), for the W/R = 0.157 baffle. It can be seen

from the SwRI tests that the minimum resonant frequency occurred

almost exactly at the point of maximum damping; the NASA results

are not so consistant in showing this behavior. In fact, the NASA

data show the minimum resonant frequency tending to occur at

baffle depths somewhat greater than that corresponding to optimum

damping.*

B.   Force Response Resulting From Liquid Sloshing in a Spherical
        Tank

1.   Description of Experimental Apparatus.   A brief description

and simplified diagram of the converted test facility was given in Ref. (1).

It is necessary, however, to describe the mounting of the ring baffles in

the spherical tank.   Six perforated ring baffles of 23% open area were

used.   These baffles were made of 0.016-in. thick perforated brass

sheet having 0.020-in. diameter holes.   They were located to form

great circles at 30° to each other.   The outer edge of the baffles was

soldered flush to the inner tank wall, of 7-1/4-in. radius.   The baffle

width was 2-1/16-in.

Tests were conducted with the baffles in two different orientations;

_____

*   Nevertheless, a statement is made in the text of Ref. (3) that
        minimum resonant frequency occurs at the point of maximum
        damping, in agreement with the SwRI data.

the horizontal orientation (B_H) is shown in Figure 4. The vertical orientation (B_V) was formed simply by rotating the sphere 90°; hence, the baffles became lines of longitude. In both cases the same cross section of the sphere, which contains one of the baffles, is perpendicular to the translational excitation axis. Hence, the axis of translation is perpendicular to the page in Figure 4.

2. Translation Excitation Results. Total force response and phase angle variation with frequency parameter are shown for both water and methylene chloride at various depths in the bare wall tank, and for water at various depths in the ring baffled tanks, for one excitation amplitude, in Figures 5-8. In addition, the vertical line in each figure shows the fundamental resonant frequency parameter $\omega_n^2 d/a$ based on results presented by NASA (8). Figure 9 shows this correlation for all of the different liquid depths considered.

As might be expected, there is essentially no difference between the dimensionless force responses for the bare wall tanks containing water and methylene chloride. It can be noted from Figure 9 that the resonant frequencies agree very well with the faired curve presented in Ref. (8), which includes two theoretical points of Budiansky (9). The fundamental resonant frequency increases with depth, until at $h/d = 7/8$ it no longer appears distinctly so that the response is more like that of a well baffled tank. It is apparent that baffles are not needed in a spherical tank for depths greater than $h/d = 3/4$, for this excitation amplitude.

The effect of changing excitation amplitude, for the bare wall configuration, is shown in Figures 10-12. Data were not consistent for depths less than $h/d = 1/2$ for the lower excitation amplitude. The resonant frequency variation with depth at the lower excitation amplitude is apparently the same as for the greater excitation. This is also shown in summary in Figure 9. It may be noted from Figure 12 ($h/d = 7/8$) that the resonant peak is still rather prominant for the lower excitation. Hence, the excitation amplitude must be considered when determining baffling requirements for depths greater than $h/d = 3/4$.

At depths where the free surface effects predominate (i. e. less than $h/d = 3/4$), both ring configurations provide pronounced damping. It can be seen that the horizontal orientation provides more damping than does the vertical orientation (Figures 6 and 7). This is expected from the location of the rings relative to the free surface, for each case. The fundamental resonant frequency, in baffled tanks, appears to be reduced to its lowest value when the damping is greatest.

No attempt was made to study other ring configurations or other geometrical variations of the ones considered. Those chosen were selected as configurations that would give considerable damping, based on experience with cylindrical tanks (5).

Pressure measurements were also obtained during the bare wall tests; however, these have not yet been completely reduced and analyzed. This data will be presented in the next Quarterly Progress Report.

3. <u>Pitching Excitation Experiments.</u> Tests for the bare wall configuration were performed with pitching excitation only for water. Force signals were too small to obtain consistent results for the baffled tank configuration. All data from these tests have not yet been reduced so that the detailed results obtained will not be presented until the next quarter.

III. PROGRAM FOR THE NEXT QUARTER

The work to be accomplished during the next quarter includes the following:

1. Complete data reduction and analysis for spherical tanks for both pressure distribution and pitching excitation.

2. Correlation of experimental data with theoretical results for intermediate depths in spherical tanks. The theoretical results will be available from research sponsored by SwRI.

3. Attempt to obtain damping factors for both baffle configurations in spherical tanks. The half band width technique used in cylindrical tanks will be employed.

4. Correlate 90° sector tank experimental data with theoretical data when the theoretical information is received from Marshall Space Flight Center.

5. Prepare such Technical Reports as may appear desirable.

REFERENCES

1. Abramson, H. Norman, Garza, L. R., and Kana, D. D., "Fuel Sloshing Studies," Quarterly Progress Report No. 1, Contract No. NAS8-1555, Southwest Research Institute, 1 July, 1961.

2. Abramson, H. Norman, Garza, L. R., and Kana, D. D., "Fuel Sloshing Studies," Quarterly Progress Report No. 2, Contract N_0. NAS8-1555, Southwest Research Institute, 1 October, 1961.

3. Silveira, M. A., Stephens, D. G., and Leonard, H. Wayne, "An Experimental Investigation of the Damping of Liquid Oscillations in Cylindrical Tanks With Various Baffles," NASA TND-715, Langley Research Center, May 1961.

4. Bauer, H. F., "Fluid Oscillations in a Cylindrical Tank With Damping," ABMA, Huntsville, Alabama, Report DA-TR-4-58, April 1958.

5. Abramson, H. Norman, "Amazing Motions of Liquid Propellants," Astronautics, pp. 35-37, 72-73, March 1961.

6. Miles, J. W., "Ring Damping of Free Surface Oscillations in a Circular Tank," Journal of Applied Mechanics, 25, 2, pp. 274-276, June 1958.

7. Armstrong, G. L. and Kachigan, K., "Stability and Control," Chapter 14, HANDBOOK OF ASTRONAUTICAL ENGINEERING, McGraw Hill Publishing Company, New York, 1961.

8. McCarty, J. L., and Stephens, D. G., "Investigation of the Natural Frequencies of Fluids in Spherical and Cylindrical Tanks," NASA TND-252, Langley Research Center, May 1960.

9. Budiansky, B., "Sloshing of Liquids in Circular Canals and Spherical Tanks," Journal Aero/Space Sciences, 27, 3, pp. 161-173, March 1960.
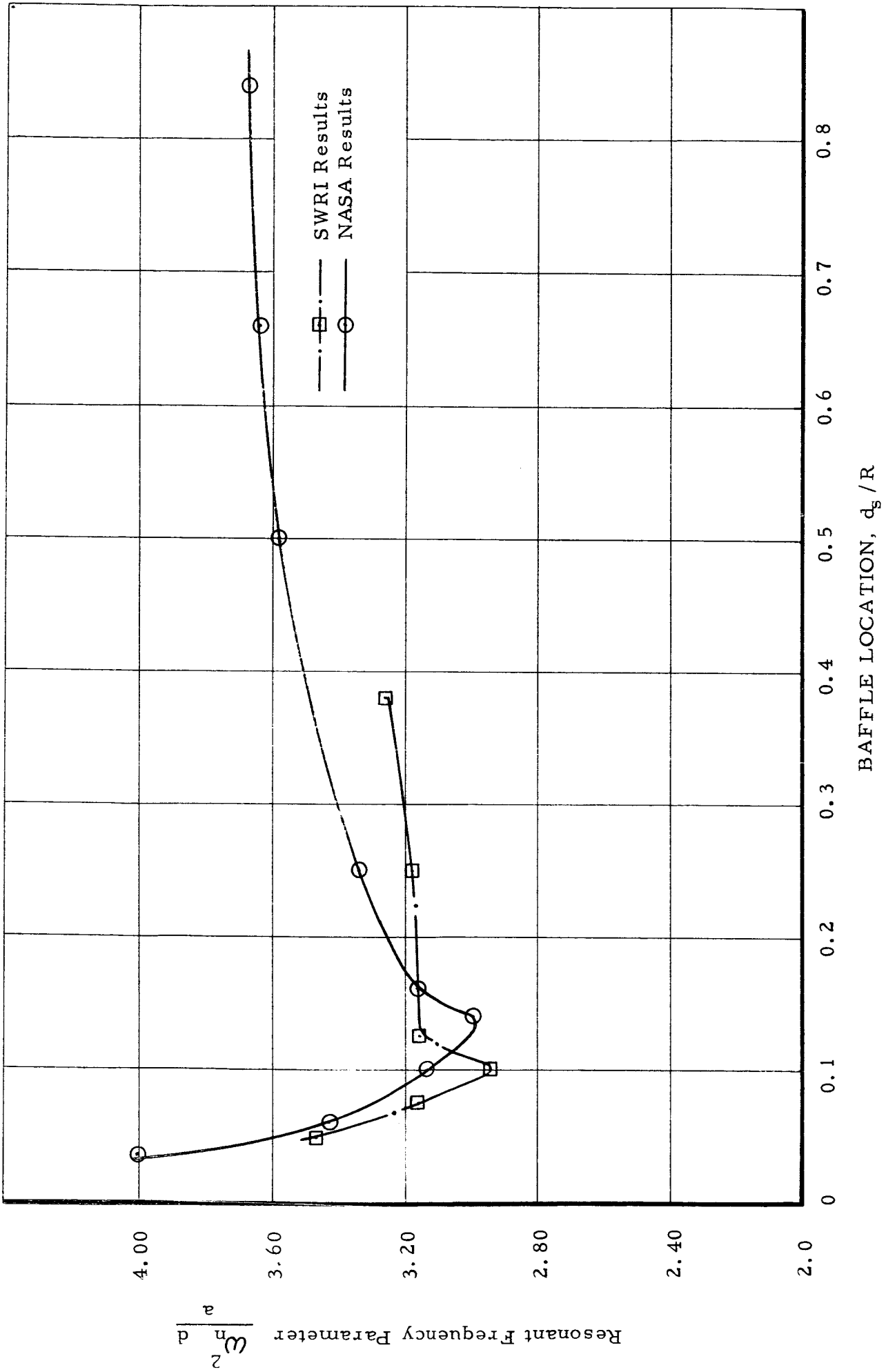
d_S

$2R$

W

R

DETAIL A
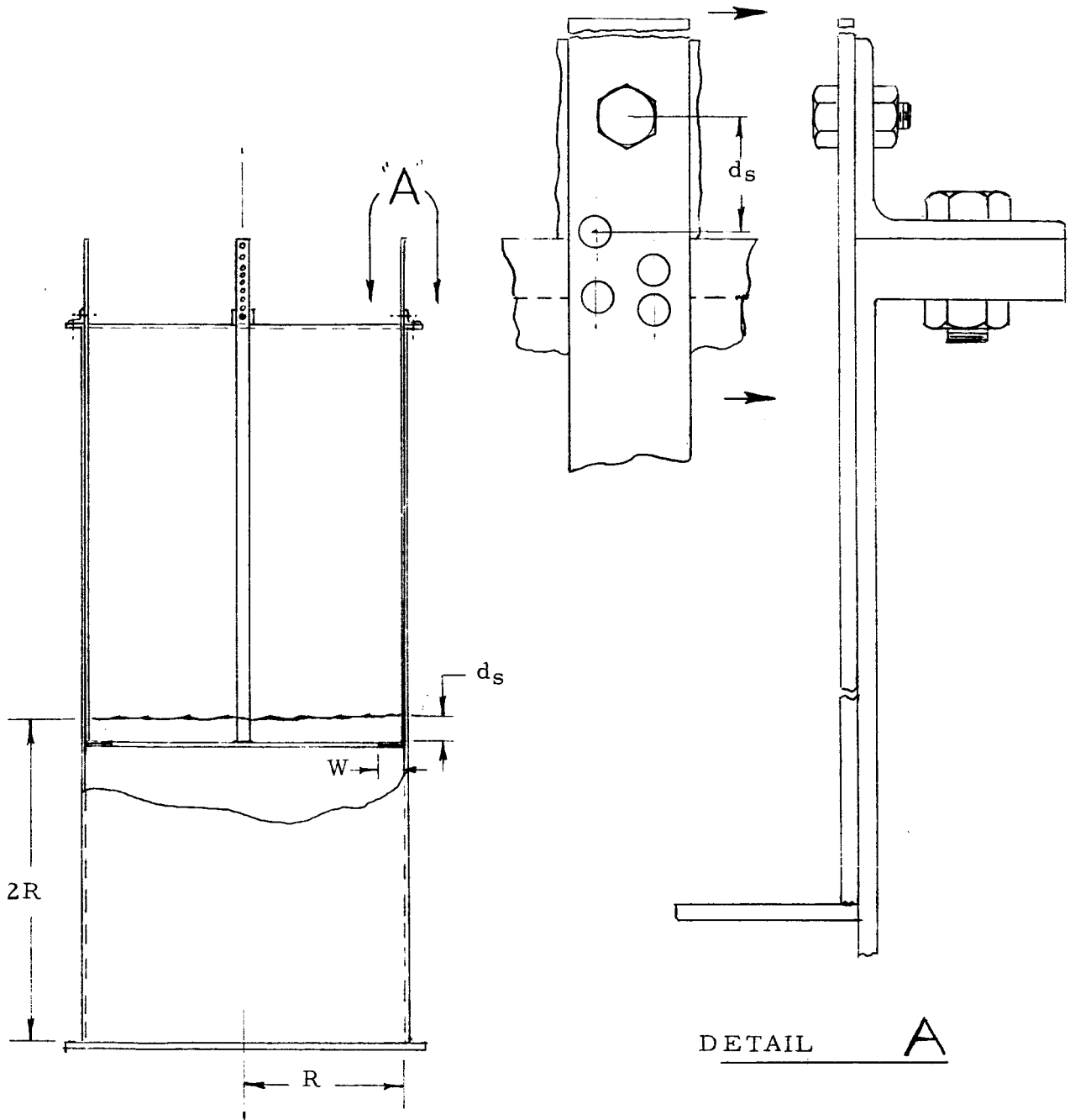
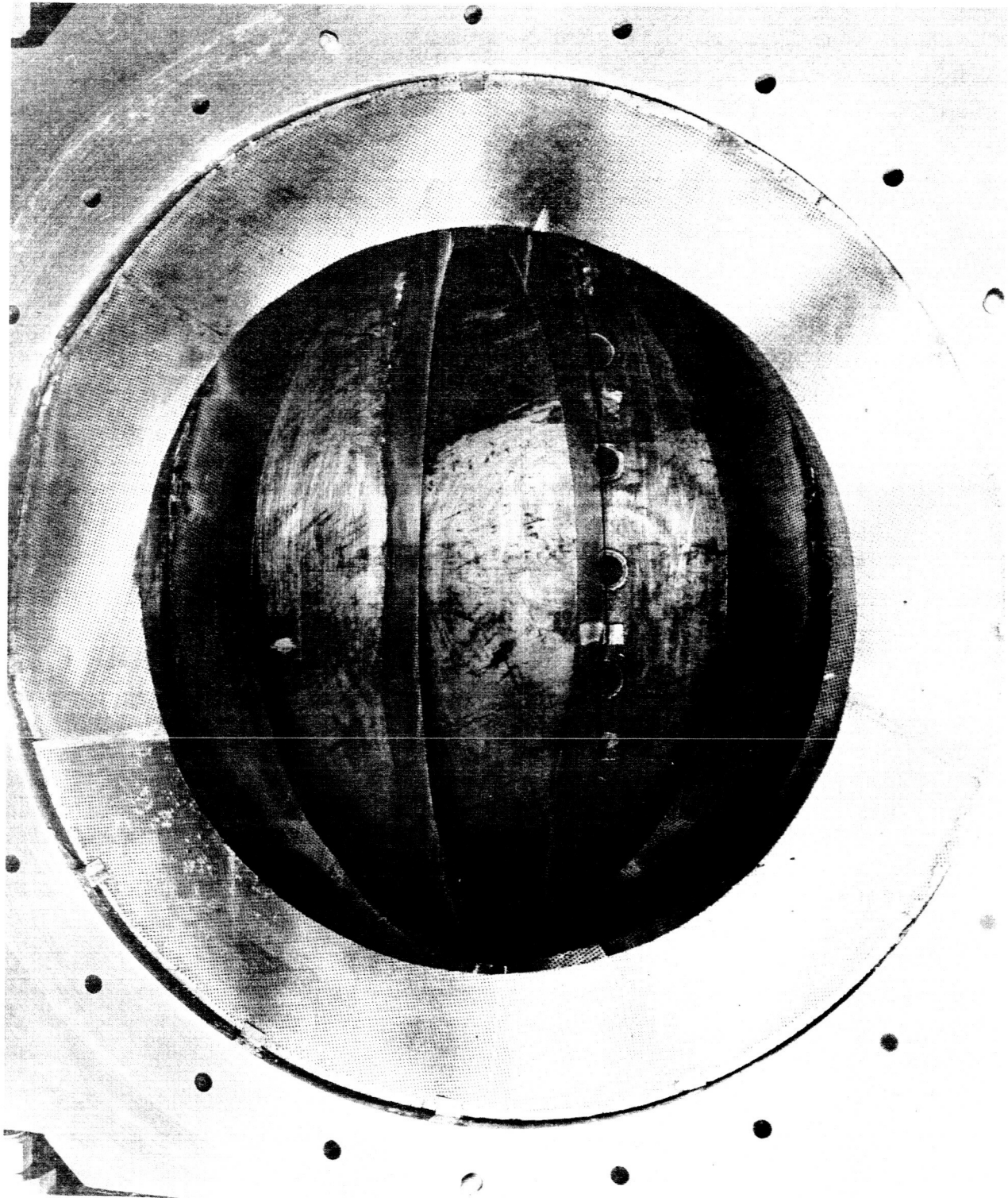RING BAFFLE SUPPORT ASSEMBLY

FIGURE 1
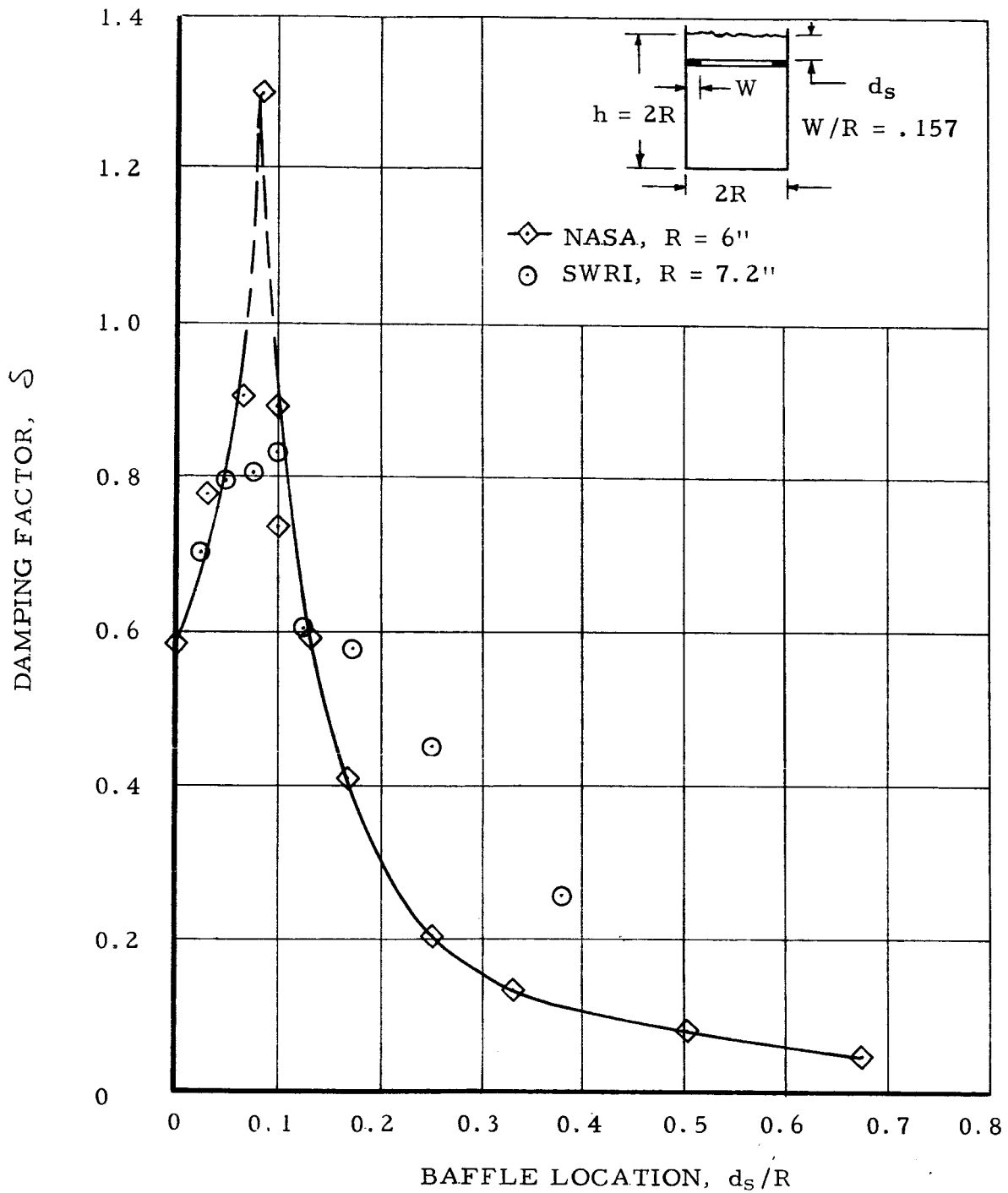
VARIATION OF DAMPING FACTOR WITH BAFFLE LOCATION

FOR FIXED-RING BAFFLE IN A CYLINDRICAL TANK

FIGURE 2

EFFECT OF BAFFLE LOCATION ON FUNDAMENTAL RESONANT FREQUENCY

FIGURE 3

HORIZONTAL BAFFLE ARRANGEMENT IN SPHERICAL TANK

FIGURE 4

TOTAL FORCE RE...
SPHERICAL TANKS BARE WALL...
$h/d = 0.250$, X_o/d...

FIGURE 5...

5-1
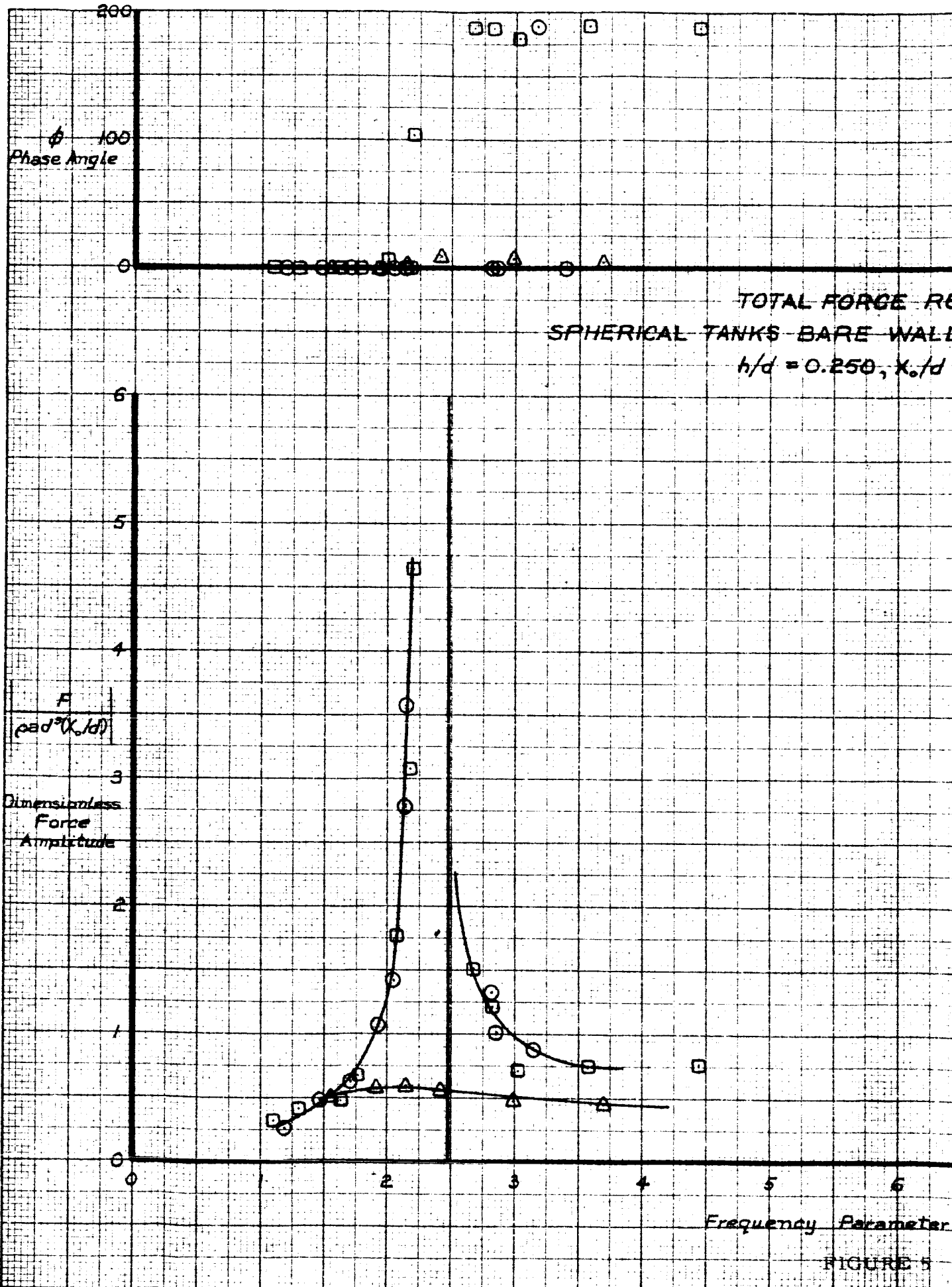
SPONSE

& FIXED RING BAFFLE

0.00828

$\oplus$ Experimental, Water, Bare Wall

$\boxplus$ Experimental, Methylene Chloride, Bare Wall

$\triangle$ Experimental, Water, Horizontal Baffle

7   8   9   10   11   12

$\omega^2 d/a$

5-2

TOTAL FORCE RE
SPHERICAL TANKS—BARE WALL
h/d = 0.500 ; X./d = 0.
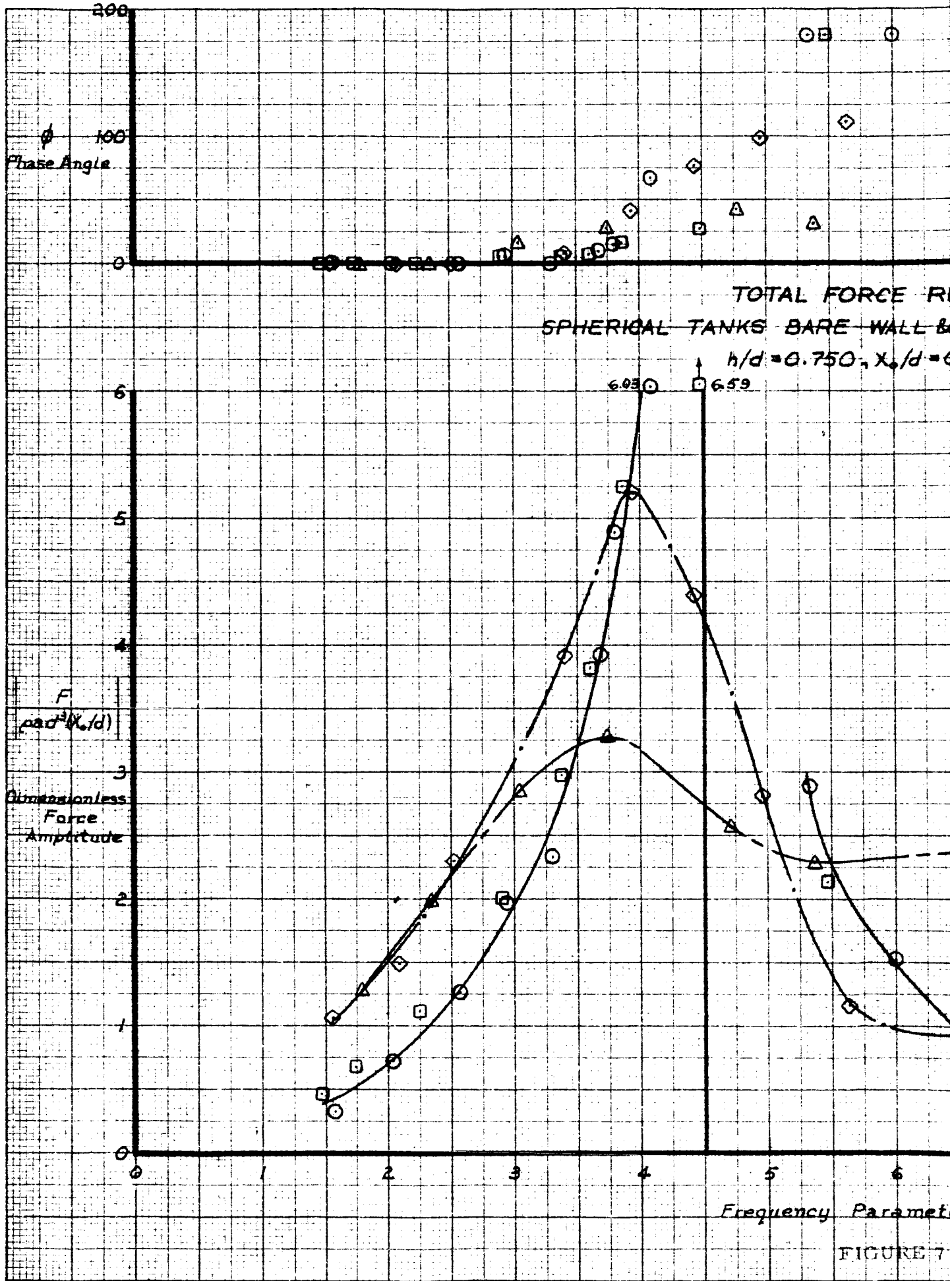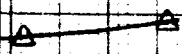
FIGURE 6

4-1

△
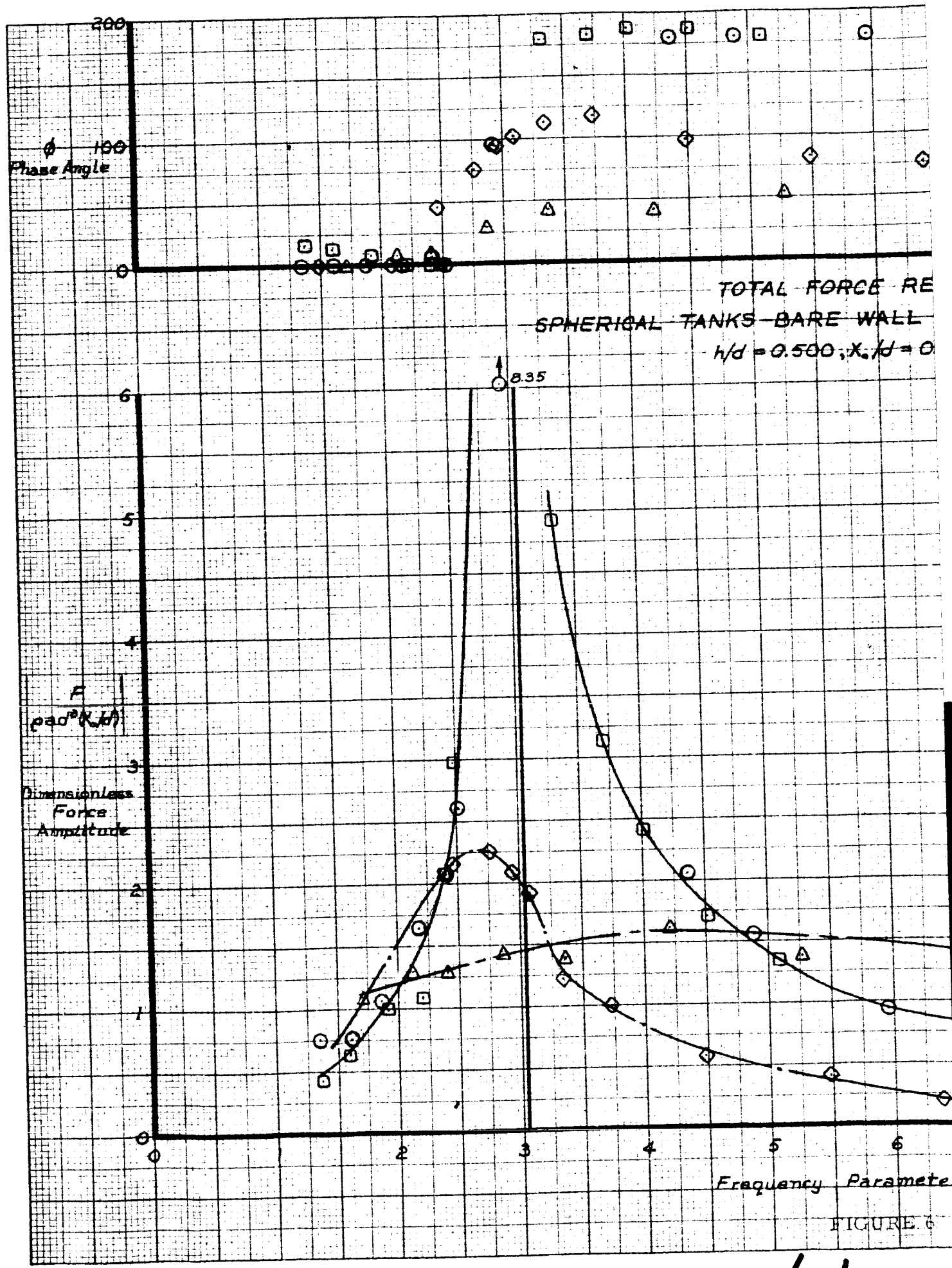
PONSE

FIXED RING BAFFLE

0828

```
——⊕——  Experimental, Water, Bare Wall
——⊟——  Experimental, Methylene Chloride, Bare Wall
——△——  Experimental, Water, Horizontal Baffle
——◇——  Experimental, Water, Vertical Baffle
```

△

7   8   9   10   11   12

$\omega^2 d/a$

6-2

TOTAL FORCE R...
SPHERICAL TANKS BARE WALL &...
$h/d = 0.750$, $X_o/d = ...$

6.03 ⊙ ⊡ 6.59

ϕ
Phase Angle

200

100

0

$\dfrac{F}{\rho a d^3 (X_o/d)}$

Dimensionless
Force
Amplitude

6

5

4

3

2

1

0

0   1   2   3   4   5   6

Frequency Paramet...

FIGURE 7...

7-1

10 X 10 TO THE ½ INCH   359-11L
KEUFFEL & ESSER CO.

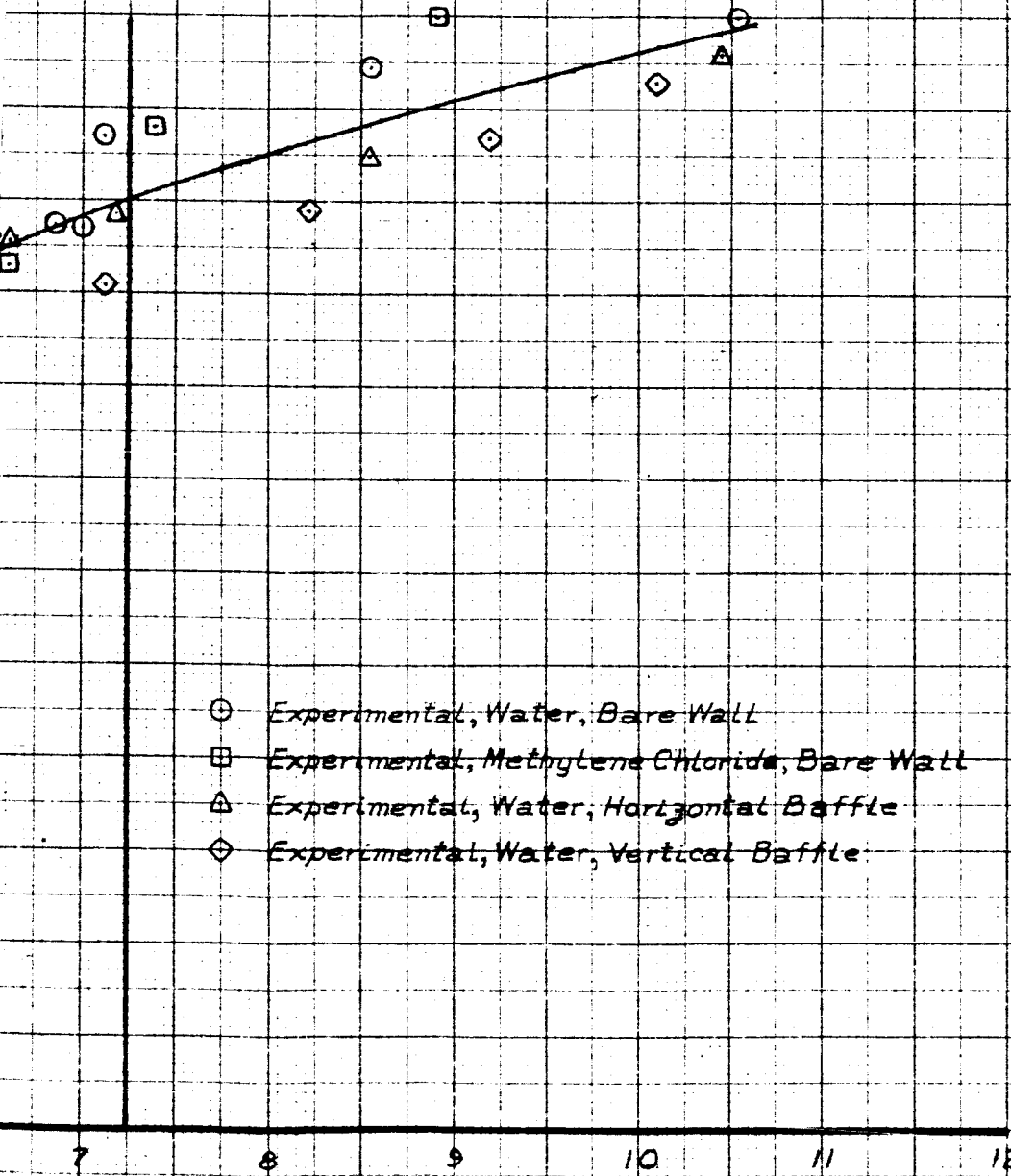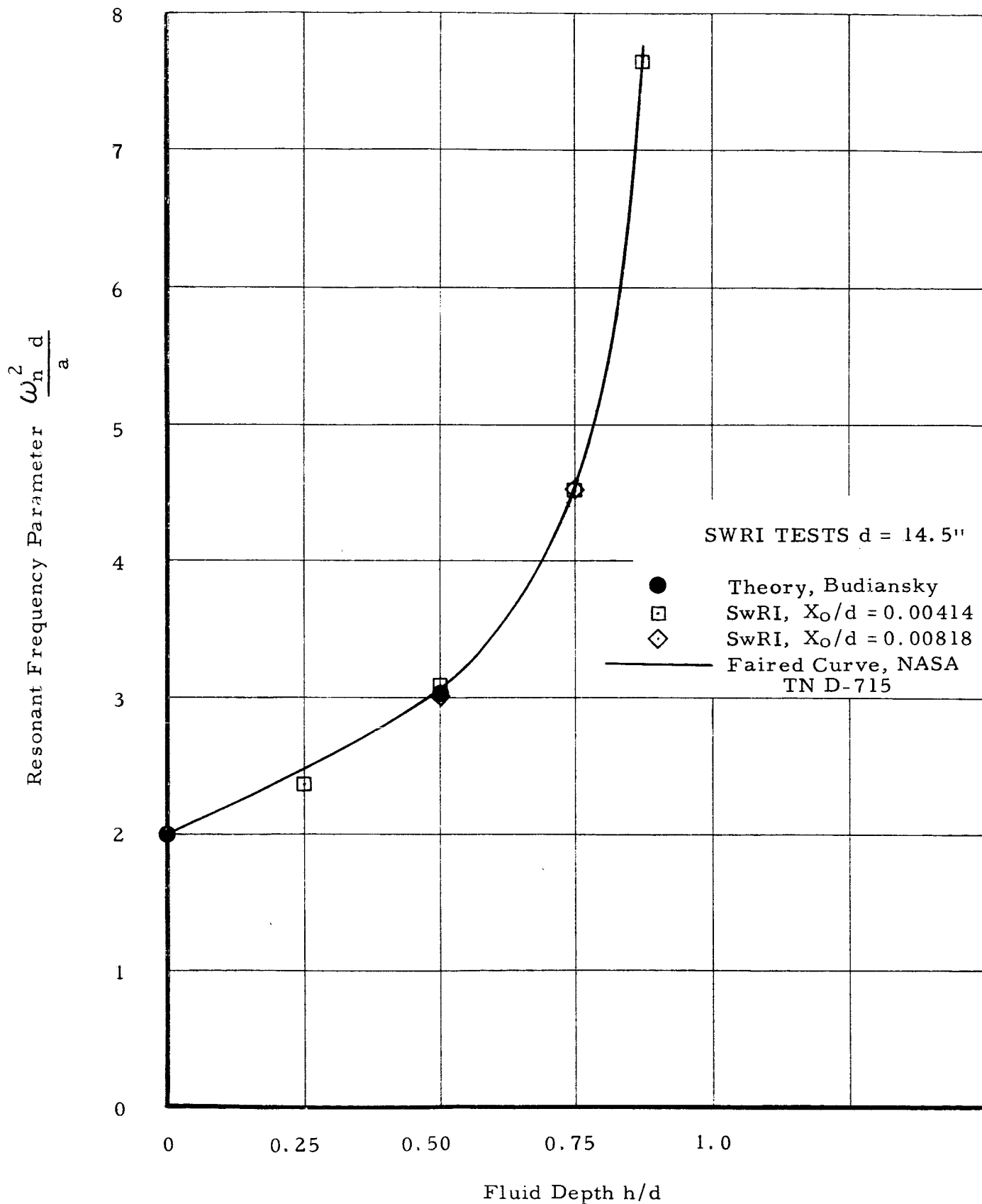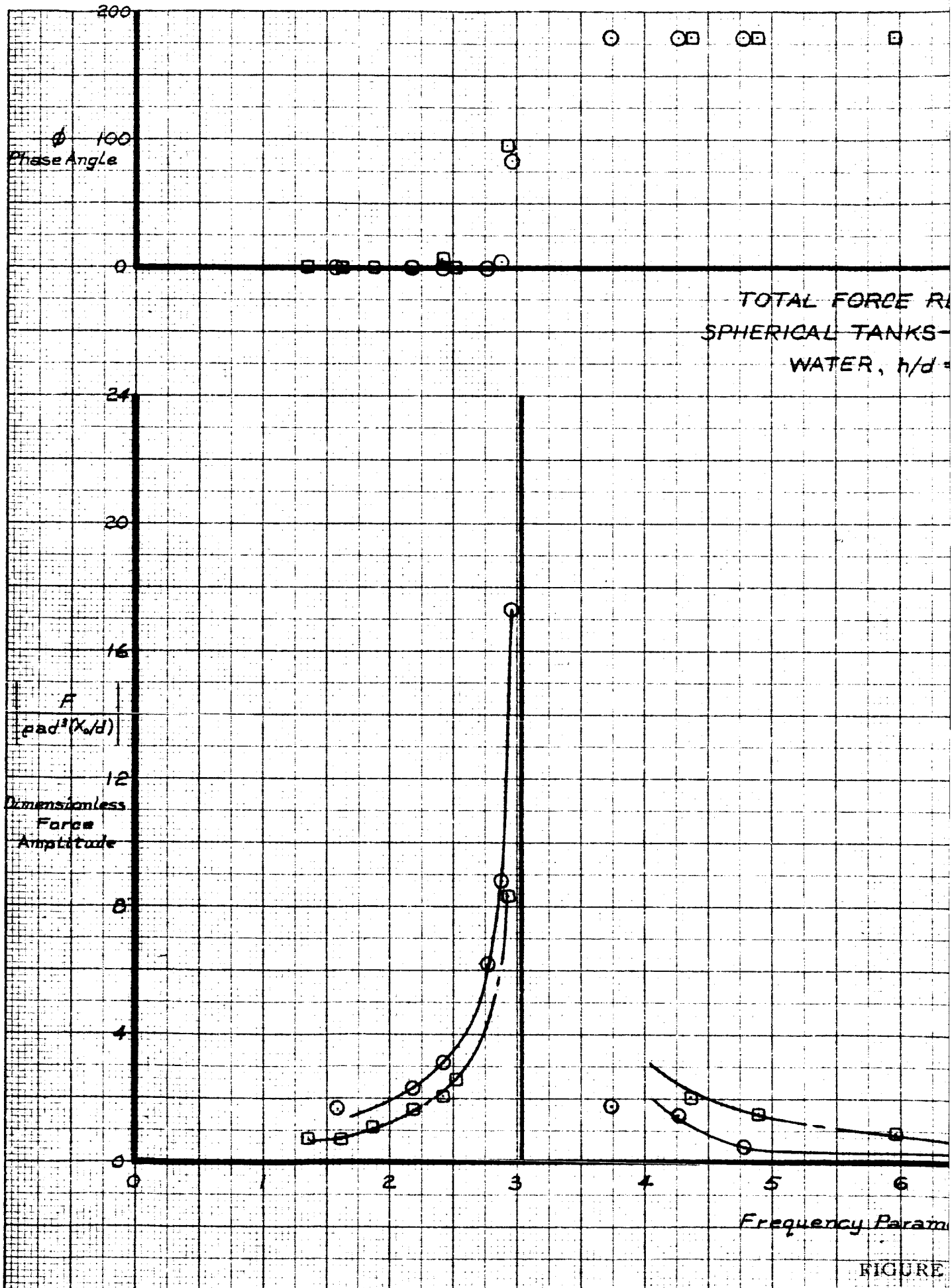SPONSE
FIXED RING BAFFLE
.00828

Experimental, Water, Bare Wall
Experimental, Methylene Chloride, Bare Wall
Experimental, Water, Horizontal Baffle
Experimental, Water, Vertical Baffle

7   8   9   10   11   12

er $\omega^2 d/a$

7-2

TOTAL FORCE RE...

SPHERICAL TANKS—BARE WALL...

$h/d = 0.875$; $X_o/d = ...$

ϕ Phase Angle

$\dfrac{F}{\rho a d^3 (X_o/d)}$

Dimensionless Force Amplitude

Frequency Parameter
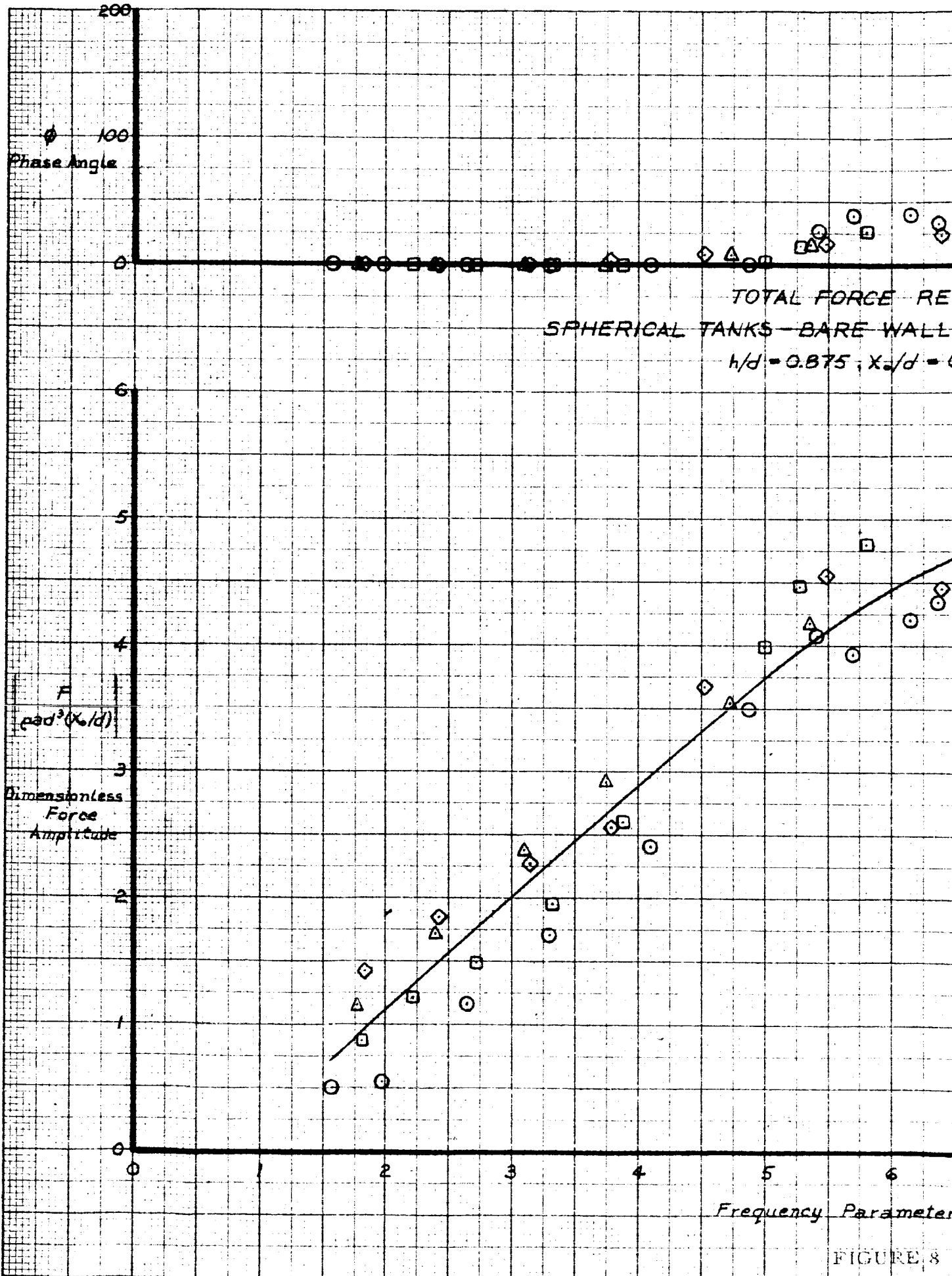
FIGURE 8

8-1

PONSE

& FIXED RING BAFFLE

00828

	Experimental, Water, Bare Wall
	Experimental, Methylene Chloride, Bare Wall
	Experimental, Water, Horizontal Baffle
	Experimental, Water, Vertical Baffle

$\omega^2 d/a$

8-2

FUNDAMENTAL RESONANT FREQUENCY PARAMETER VARIATION
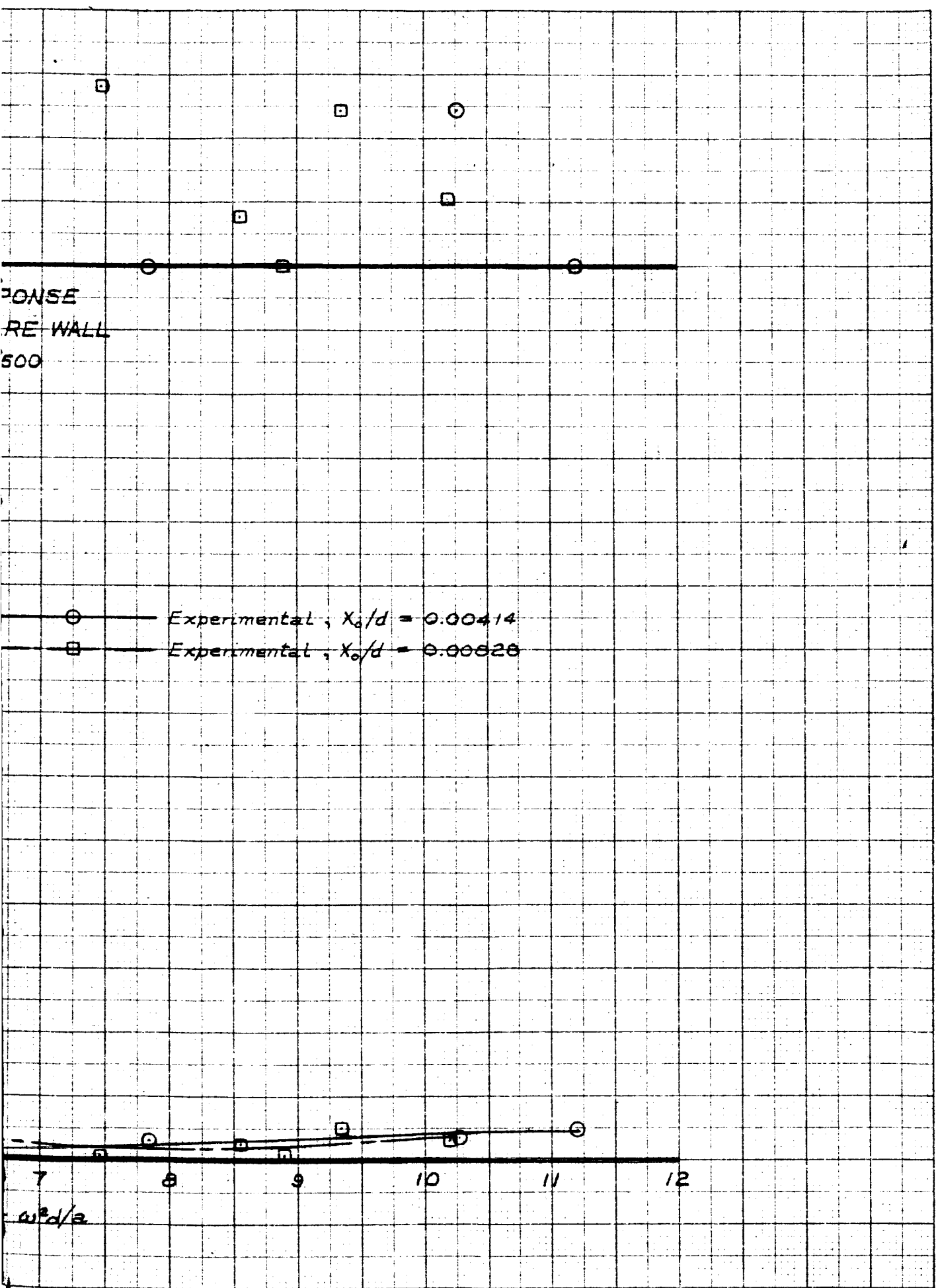
WITH DEPTH FOR SPHERICAL TANKS

FIGURE 9

TOTAL FORCE R...
SPHERICAL TANKS—
WATER, h/d =

Frequency Param...

FIGURE

10-1

PONSE
RE WALL
500

Experimental , $X_0/d = 0.00414$
Experimental , $X_0/d = 0.00828$

7   8   9   10   11   12

$\omega^2 d/2$

10-2

TOTAL FORCE RE
SPHERICAL TANKS—
WATER, h/d = 0.

FIGURE

11-1

PONSE
RE WALL

○

———⊕——— Experimental, $X_0/d = 0.00414$
———⊟——— Experimental, $X_0/d = 0.00828$

7   8   9   10   11   12

$\omega^2 d/a$

11-2

TOTAL FORCE RE
SPHERICAL TANKS—
WATER, h/d = 0

Experimental, X_o/d = 0.00414
Experimental, X_o/d = 0.00028

ϕ
Phase Angle

$\dfrac{F}{\rho a d^3 (X_o/d)}$

Dimensionless
Force
Amplitude

Frequency Parame

FIGURE

ONSE

RE WALL

5

$\omega^2 d/a$

12-2